ACADEMIC PRESS

Available online at www.sciencedirect.com

SCIENCE DIRECT®

Journal of Magnetic Resonance 161 (2003) 56–63

JMR Journal of Magnetic Resonance

www.elsevier.com/locate/jmr

Selective polarization inversion of protons in rotating solids

Gil Goobes, Elena Vinogradov, and Shimon Vega*

Department of Chemical Physics, Weizmann Institute of Science, Rehovot 76100, Israel

Received 10 July 2002

Abstract

The selective inversion of lines under phase modulated Lee–Goldburg (PMLG) decoupling in MAS proton spectroscopy is demonstrated. Short pulses inserted between consecutive PMLG irradiation intervals selectively invert the polarization of an on-resonance line while sustaining a high resolution proton evolution. The pulse scheme is combined with windowed-PMLG detection to obtain a one-dimensional high resolution spectrum with one of the proton lines inverted. Initial preparation of the protons in selectively inverted states can be used to follow the flow of polarization during spin diffusion. Examples of proton–proton spin exchange in alanine and histidine are demonstrated. Selective inversion is also used in conjunction with proton carbon LG-cross-polarization to achieve carbon spectra with lines characterized by different polarization states.

Keywords: Proton spectroscopy; Selective inversion; DANTE; PMLG; MAS

1. Introduction

Hydrogen atoms serve as primary NMR probes due to their high abundance in organic and bio-organic materials and their large nuclear magnetogyric ratio. The high sensitivity and resolution of proton spectroscopy of liquids at high magnetic fields makes it an important component of protein-NMR structure determination. In solids, protons form large networks of strongly dipolar coupled spins characterized by broad spectral lines. The nuclear dipole–dipole interactions in these networks can be five orders of magnitude larger than the residual spin–spin interactions in solution, posing a great challenge to the attainment of ''high resolution'' proton spectra. The most widely used line narrowing technique in solid state NMR is magic angle spinning (MAS) [1–3], in which the sample is rotated about an axis inclined at an angle of 54.7° with respect to the external magnetic field. This technique can be used to achieve line narrowing, but requires, in the case of protons, ultra-high spinning frequencies, exceeding the largest dipole–dipole interaction strength, to obtain high resolution spectra [4–6]. In addition to MAS, homonulcear r.f. decoupling schemes that were developed through the years, can be used for effective elimination of the dipole–dipole interaction. The Lee–Goldburg (LG) [7] decoupling scheme using off-resonance irradiation and its contemporary versions frequency switched LG(FSLG) [8–11] and phase modulated LG (PMLG) [12,13], the multiple pulse schemes like WHH-4 [14], MREV-8 [15,16], BR24 [17], and MSHOT-3 [18], as well as the composite pulse irradiation DUMBO [19,20] can all be combined with sample spinning. The combination of r.f. irradiation and MAS (CRAMPS) has proven to achieve the best resolved proton spectra of powdered solids [21–24]. However, such a combination with high speed MAS requires special attention, since most of the pulse techniques were developed for non-rotating samples. Schemes like FSLG and PMLG have the advantage of being composed of short repeating time units and, hence, can be combined successfully with relatively high spinning frequencies [5,13,19,25,26]. It was recently shown that acquisition windows can be inserted in the PMLG and FSLG pulse schemes, enabling one-dimensional detection of high resolution proton spectra [27,28]. These experiments have motivated the introduction of the composite DANTE-PMLG experiment.

The DANTE pulse experiment [29] employs a series of equally spaced pulses with small flip angle to selectively invert lines within a set of narrow frequency

* Corresponding author. Fax: +972-8-934-4123.
E-mail address: shimon.vega@weizmann.ac.il (S. Vega).

1090-7807/03/$ - see front matter © 2003 Elsevier Science (USA). All rights reserved.
doi:10.1016/S1090-7807(02)00135-0

windows in the spectra. The width of these excitation windows is inversely proportional to the pulse strength and similarly the separation between windows is inversely proportional to the time between the pulses. The DANTE sequence can thus be tuned to exclusively affect a single line in a high resolution spectrum. In solid samples under MAS conditions the DANTE pulse train was used to invert partial and full sideband manifolds [30]. In the DANTE-selective-REDOR (DSR) pulse experiment it was utilized to promote selective homonuclear dipolar recoupling [31] and in the C7 experiment [32], carried out on fully ^{13}C-labeled samples, it was used in the preparation period to hinder the recoupling of specific dipolar coupled spin pairs [33]. It was also employed in 2D exchange measurements to excite parts of deuterium powder spectra [34] and for line assignments in conjunction with REDOR [35]. Narrow spectral selectivity was additionally utilized in solid state magnetic resonance imaging [36]. The exchange of longitudinal magnetization in a pair of dipolar coupled spins, driven by a zero-quantum (ZQ) dipolar Hamiltonian, is most efficient when the pair is prepared with opposite spin polarization. This is the case in experiments such as R^2 [37], RFDR [38], spin diffusion [39], and others [40]. Techniques that employ polarization transfer, such as one-dimensional cross-polarization experiments, could benefit from selective line inversions when coupled heteronuclear spin pairs must be identified during spectral editing.

Polarization and coherence exchange in strongly coupled proton systems is very fast. In the non-irradiated intervals of the DANTE sequence the individual spin coherences redistribute, destroying chemical shift selectivity. Thus to use DANTE inversion, one must maintain the spins in a decoupled state during the time between its pulses. The combination of MREV-8 [15,16] homonuclear decoupling with selective line inversion was reported by Caravatti et al. [41]. It was employed in inversion recovery and saturation transfer spin diffusion experiments to verify the presence of mixed domains in polymer blends [42]. Lately it was shown that phase modulation of the PMLG decoupling scheme can as well be used to obtain selective inversion [43]. This was achieved by employing a Gaussian envelope to the PMLG irradiation field in the decoupling interaction frame.

In this publication it is demonstrated that short DANTE pulses can be appended to the PMLG decoupling cycle in order to obtain line inversions in solid state proton spectra. The PMLG spin evolution between these pulses distinguishes on-resonance lines from off-resonance lines, necessary for the selective inversion. The PMLG irradiation is associated with an effective chemical shift Hamiltonian that is pointing in a direction subtended by an angle of 54.7° with respect to the external magnetic field. Thus during these intervals the spins experience scaled chemical shift interactions. The relatively short cycle time of the PMLG sequence provides flexibility in the choice of decoupling intervals of the DANTE scheme. This short cycle time, that is in general asynchronous with the sample spinning, is especially favorable when inversion experiments are performed at high spinning rates. In the following section the essential parameters for the combined DANTE-PMLG experiment are presented and numerical simulations demonstrating the efficiency of the inversion scheme are shown. Results of selective inversion experiments on uniformely ^{13}C, ^{15}N enriched and non-enriched samples of histidine are shown and the use of the pulse sequence in combination with proton–proton spin diffusion measurements and ^{1}H–^{13}C Lee–Goldburg-cross-polarization (LG-CP) experiments [44] is demonstrated.

2. The DANTE-PMLG pulse sequence

The DANTE-PMLG pulse scheme for selective line inversion is shown in Fig. 1a. It is composed of basic

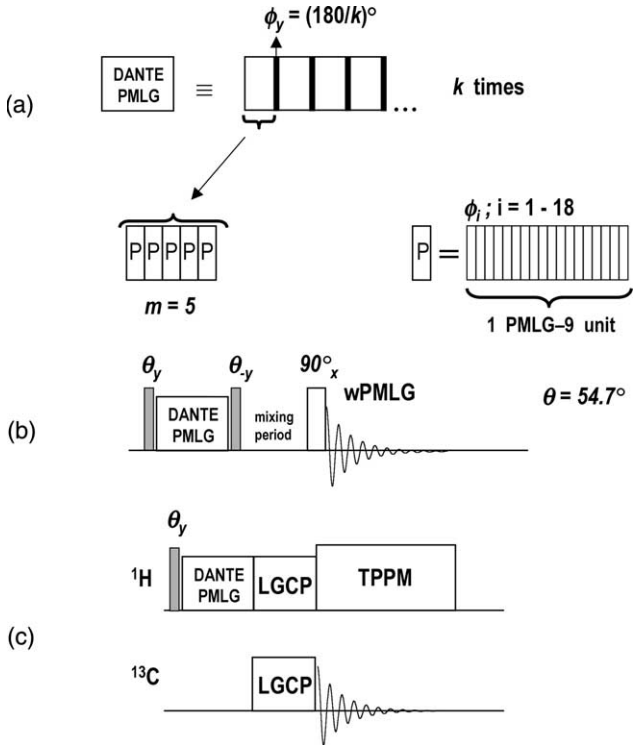

Fig. 1. (a) The DANTE-PMLG irradiation scheme for selective polarization inversion during PMLG decoupling. Each DANTE pulse of length $(180/k)°$ is adhered to a decoupling block consisting of m integer PMLG-9 units (P) and is repeated k times to achieve full inversion. (b) The combination of selective inversion with 1D high resolution wPMLG acquisition. (c) Selective proton inversion in conjunction with LG cross-polarization. A LG cross-polarization field is exerted by off-resonance irradiation of the protons at the LG condition and on-resonance irradiation of the carbons. Carbon signal is acquired under TPPM decoupling.

blocks containing a set of PMLG-n units followed by a short DANTE pulse. This block is repeated k times, where k is an integer denoting the ratio of 180° and the pulse tilt angle ϕ_y, $k = 180°/\phi_y$. The decoupling interval between the DANTE pulses spans an integer number m of PMLG-n units. In the experiments conducted n was taken equal to 9, requiring 18 pulses during each PMLG unit with phase values given in Table 1. The number of PMLG-9 units per block was either $m = 5$ or $m = 10$. Assuming that the PMLG irradiation eliminates the homonuclear dipolar interaction between the protons, the effective Hamiltonian that governs proton evolution is a scaled chemical shift Hamiltonian. During the PMLG irradiation intervals, the proton coherences effectively nutate around a field associated with the chemical shift Hamiltonian. The effective nutation frequencies are equal to the chemical shift values of the protons $\Delta\omega_i$ scaled by a constant factor, $s \simeq 0.57$. Proton evolution can thus be evaluated using an effective chemical shift Hamiltonian in the PMLG interaction frame

$$\overline{\mathcal{H}} = s\sum_i \Delta\omega_i(I_{zi}\cos\theta_m + I_{xi}\sin\theta_m), \tag{1}$$

where it is assumed that the carrier frequency of the PMLG irradiation points in the x direction of the rotating frame. In analogy to a standard DANTE experiment the inversion pulses should point in a direction perpendicular to the effective chemical shift Hamiltonian which was chosen to be parallel to the rotating frame y direction. The evolution of proton magnetizations with different chemical shifts during the DANTE-PMLG experiment is thus equivalent to the evolution during a standard DANTE experiment. The differences being the scaling coefficient and the tilt of the effective chemical shift Hamiltonian. In the experiments presented hereafter the length of the DANTE pulses was 0.37 μs, corresponding to a flip angle of 16.4°, and the decoupling intervals were 99.0 μs ($m = 5$) and 198.0 μs ($m = 10$) long. These lengths as well as the PMLG r.f. phase discretization can be varied to optimize the selectivity and decoupling efficiency in the experiment. The inversion pulse sequence is combined with windowed-PMLG (*w*PMLG) data acquisition [27] for the detection of individual inversion of lines (see Fig. 1b).

Table 1
Experimental parameters

Spinning frequency	14 kHz
Preparation	
54.7° pulses	1.95 μs
PMLG r.f. power	$\nu_1 = 81.6$ kHz
PMLG unit length	19.8 μs
PMLG phases	11.54° → 196.26° (9 steps of 23.08°)
	16.26° → −168.46° (9 steps of −23.08°)
# of DANTE pulses	11
DANTE pulse length	0.37 μs
Detection	
90° pulse	4.5 μs
*w*PMLG r.f. power	$\nu_1 = 81.6$ kHz
*w*PMLG phases	20.78° → 187.02° (5 steps of 41.56°)
	7.02° → +200.78° (5 steps of −41.56°)

To start the inversion sequence, an initial 54.7° y-pulse must be applied to align the spin magnetization along the effective PMLG field direction. The selective DANTE-PMLG pulse scheme is then applied at the frequency of one of the lines, inverting the protons of this line and leaving the rest of the system in the PMLG field direction. The pulse sequence is then followed by a flip-back y-pulse of −54.7° transferring the magnetizations back to the $\pm z$ direction. The chemical shift scaling factor of the PMLG decoupling scheme was $s = 0.575$. After the DANTE-PMLG sequence and prior to *w*PMLG signal acquisition, the carrier frequency is shifted out of the spectrum and a 90° x-pulse is applied to orient the magnetizations perpendicular to the effective *w*PMLG field direction. During proton spin diffusion experiments, a variable mixing period, devoid of r.f. irradiation, was inserted between the flip-back pulse and the 90° pulse. The DANTE-PMLG selective proton line inversion was additionally used as a preparation stage for proton–carbon spectral editing, using LGCP transfer. In this case a line in the proton spectrum is inverted followed by a standard LGCP experiment that monitors the buildup of carbon signals as a function of the CP mixing time. In these experiments, the flip-back pulse is omitted and the *w*PMLG acquisition period in Fig. 1b is replaced by a LGCP proton–carbon irradiation period terminated with carbon signal detection (Fig. 1c).

3. Simulations

Simulations on a system of four protons were carried out, modeling a HOOC–CH_2–CHD_2 molecule with off-resonance values 9.8, 3.8, and 2.3 kHz, respectively. The simulations employed full density matrix calculations, using the SIMPSON [45] simulation program. The inversion of the individual lines was achieved, using an r.f. irradiation at a power level of 81.6 kHz for the PMLG decoupling and the DANTE pulses. The inter-pulse decoupling intervals consisted of five PMLG-9 cycles. For signal simulations PMLG-9 decoupling at the same r.f. power level was assumed between the acquisition points. In Fig. 2, the results of the DANTE-PMLG inversion are plotted. The top spectrum displays the 1D PMLG decoupled proton spectrum of the model molecule and the lower two spectra show selectively inverted spectra, one with inversion of the CH_2 line at 3.8 kHz and the other with inversion of the carboxyl line at 9.8 kHz. Inversion of the carboxyl proton did not affect the intensities of the two other proton lines, while

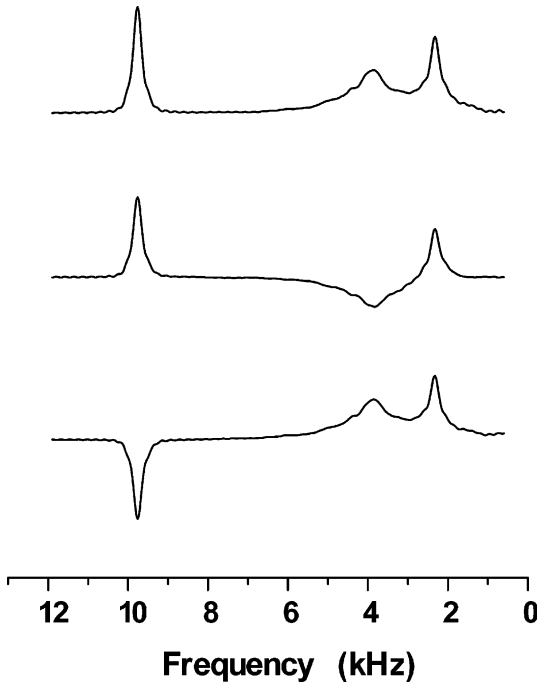

Fig. 2. Results of inversion simulations carried out using the model molecule HOOC–CH_2–CHD_2 are shown in this figure. The top figure shows the 1D proton spectrum of the molecule. The signal was calculated with PMLG-9 decoupling between the sampling points. The middle spectrum shows inversion of the CH_2 protons and the bottom spectrum shows inversion of the carboxy protons. Both simulations were carried out using the DANTE-PMLG sequence with decoupling blocks of $m = 5$ PMLG-9 units at a field of 82 kHz. The sequence was repeated $k = 11$ times for full inversion of the proton polarization.

inversion of the CH_2 protons causes an intensity loss of both the inverted line and the adjacent CH line. These results imply that the dipolar interactions are not eliminated completely during the DANTE-PMLG irradiation and ideal selective inversion cannot be achieved. However, imperfections are small enough to make it experimentally accomplishable.

4. Experimental

Samples of uniformly ^{13}C (98%), ^{15}N (96–99%)-labeled L-histidine · HCl · H_2O (U-histidine) salt and of 2-^2H (98%)-labeled DL-alanine were purchased from Cambridge Isotope Laboratories, MA. A sample of non-labeled L-histidine · HCl · H_2O (NA-histidine) salt was purchased from Sigma. All samples were used as purchased. The DANTE-PMLG experiments employed pulse parameters as summarized in Table 1. A total of $k = 11$ DANTE pulses were used to achieve inversion spanning total irradiation periods of 1093.0 μs for $m = 5$ and 2182.0 μs for $m = 10$, respectively. The *w*PMLG-5 scheme was used for the 1D proton detection. During the *w*PMLG acquisition the carrier frequency was shifted away from the spectrum so that it would not coincide with any of the lines. Only the low-field part of the spectra is displayed in the proton spectra. All experiments were carried out on a standard Bruker DSX300 spectrometer. The proton detected experiments were performed with a 4 mm CRAMPS probe and with a 4 mm triple-tuned MAS probe, both from Bruker. The phase switching time of the spectrometer is of the order of 0.06 μs. Acquisition windows of 3.2 μs and of 4.9 μs were used for the CRAMPS probe and for the triple-tuned MAS probe, respectively, to collect the *w*PMLG-5 decoupled proton signals. No significant decoupling deterioration was observed in the spectra recorded on the triple-tuned probe as compared to the CRAMPS probe. Carbon detected experiments were carried out using the triple-tuned MAS probe.

In the selective line inversion experiments as well as in the alanine spin diffusion experiments a spinning frequency of 14 kHz was employed. In the histidine spin diffusion experiment and in the spectral editing experiments spinning frequencies of 10 and 11 kHz were used, respectively. All pulse-lengths were optimized to achieve the best resolution while minimizing the zero-frequency lines in the spectra. The frequency axes of experimental spectra were divided by the scaling factor (0.575) in order to present proton spectra along standard ppm axes. The procedure of tuning the inversion sequence involves initial optimization of the PMLG decoupling scheme [12]. This pulse scheme is quite robust delivering almost no decoupling degradation with variation of 10% in r.f. power. The initial magic pulse is set by recording the phase of an on-resonance line as a function of the PMLG lock time. The requirement of no phase change at extended lock times enables to accurately direct the magnetization along the effective PMLG field axis. An additional experiment that employs preparation of the protons along the *y*-direction (perpendicular to the PMLG field) is used to cross-check that the PMLG field is aligned along the magic angle direction. This is done by recording the relative phase accumulation, ϕ_{rel}, of a line with off-resonance frequency, ν_H, as a function of the PMLG time and extracting the scaling factor, s, from measurements at two off-resonance values ($\phi_{rel} = s \cdot \nu_H t$). The DANTE-PMLG scheme is then optimized by choosing the shortest possible duration for the inversion pulses with an angle that is a submultiple of 180° and by determining the number of inter-pulse PMLG blocks necessary for preservation of the decoupling efficiency. For the LGCP transfer measurements the DANTE-PMLG scheme was used in the preparation period. All parameters used in the initial inversion step of this experiment were the same as in the proton detected experiments. The LGCP contact time was 200.0 μs and the r.f. intensities of the proton and carbon channels were $\omega_{1H} = 72$ kHz and $\omega_{1C} = 99$ kHz, respectively. TPPM decoupling using an r.f. field strength of 90 kHz was exerted on the protons during carbon acquisition.

5. Results

The *w*PMLG proton spectrum of U-histidine after a single $\pi/2$ excitation is shown in Fig. 3a and compared with spectra collected after a spin-locked PMLG and a DANTE-PMLG preparation period of 1089.0 and 1093.0 μs, respectively, in Figs. 3b and c. In these 1D spectra five resolved bands can be distinguished. The two low-field lines at 16 and 12 ppm are due to the amine (–NH) protons in positions 2 and 4 on the ring, respectively (see insert). The large band at 8 ppm with small shoulders on each side consists of contributions from the NH_3^+ protons and the CH protons in positions 3 and 5 on the ring. The protons of a water molecule present in the crystal phase appear at 4 ppm and the α-CH and β-CH_2 protons at 2 ppm. The relative integrated intensities of the five bands in Fig. 3a, with decreasing ppm values, are 1.0:1.0:4.7:1.0:3.2(±0.2). These values follow the number of protons in each band, except for the intensity of the water line which is significantly reduced. It is apparent that signal losses (~40%) in the inversion experiment in Fig. 3c are mainly due to depletion of polarization during the spin-locking PMLG sequence itself, as can be seen in Fig. 3b. This indicates that the inter-leaved DANTE pulses themselves have a small effect on the intensities and widths of the lines. In Figs. 4a–d *w*PMLG spectra following selective DANTE-PMLG inversion are shown. The different lines were inverted merely by shifting the carrier frequency of the DANTE-PMLG irradiation between consecutive experiments. Except for the last spectrum shown in Fig. 4d, where decoupling intervals of $m = 10$ PMLG-9 units were inserted between the DANTE pulses, all spectra were collected using decoupling intervals of $m = 5$ PMLG-9 units.

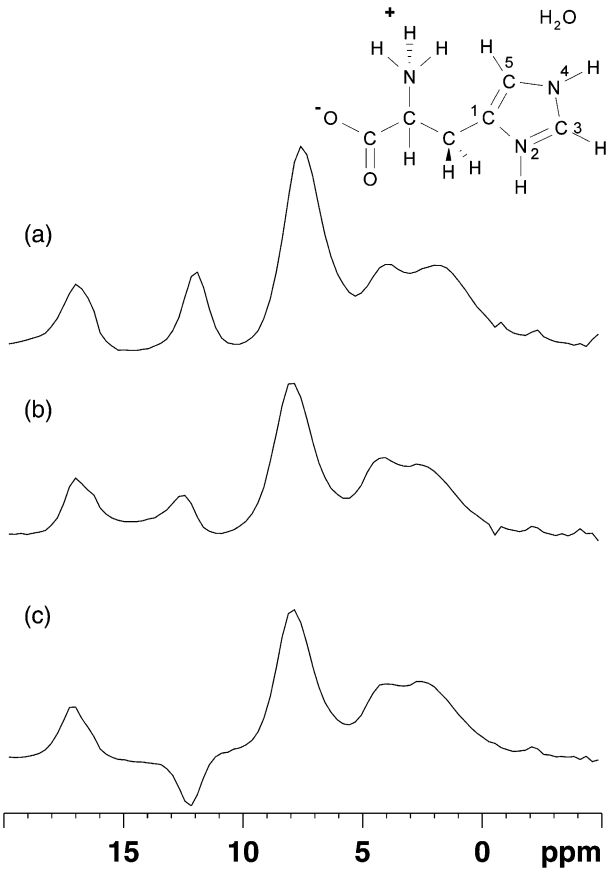

Fig. 3. Comparison between U-histidine spectra obtained from free induction decay signals measured during *w*PMLG (a) after a single $\pi/2$ *y*-pulse, (b) after a PMLG spin locking period, and (c) after a DANTE-PMLG selective inversion. The PMLG and DANTE-PMLG intervals employed $k = 11$ PMLG-9 blocks of 99.00 and 99.37 μs each, respectively.

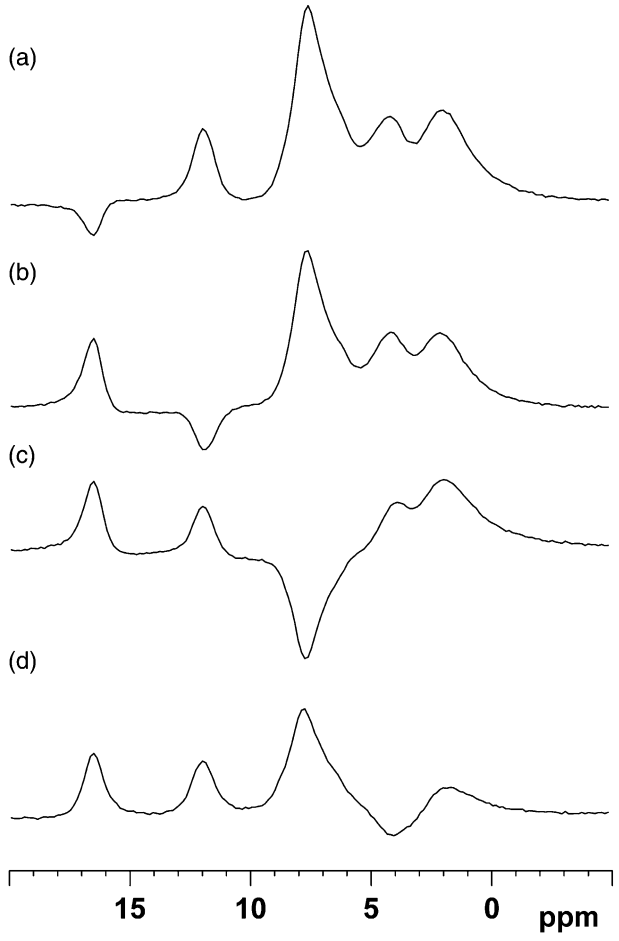

Fig. 4. Experimental results of selective inversion of individual proton lines in spectra of U-histidine. *w*PMLG signals were detected and Fourier transformed after a DANTE-PMLG inversion applied at offset values (a) 1350 Hz, (b) 0 Hz, (c) −1250 Hz, and (d) −2750 Hz, relative to the frequency of the 8 ppm line maximum. For the experiments shown in (a–c) the DANTE-PMLG sequence was comprised of $m = 5$ PMLG units per short DANTE-pulse, and for (d) $m = 10$ units were inserted between the short pulses to enhance the selectivity. In all experiments a total of $k = 11$ DANTE-pulses of length 0.37 μs and a total inversion time of 1093.0 μs were employed except for the last experiment with total inversion time of 2182.0 μs. The number of signal accumulations for each spectrum was 64.

After inversion of one of the lines in the spectrum proton–proton spin diffusion brings about internal equilibrium of the proton spin bath, and spin lattice relaxation returns this bath to thermal equilibrium with the lattice. In Fig. 5, the time dependence of the integrated intensities of selectively inverted *w*PMLG spectra as a function of the proton–proton spin diffusion length in the experiment are presented. In Fig. 5a, the results of spin diffusion between the initially inverted NH_3^+ and the CH_3 protons in 2-[^{2}H]alanine are summarized. Only the short time dependence of the two proton polarizations is shown. Two internal euqilibrium decay rates, 714 and 7812 s^{-1}, can be derived from a bi-exponential fitting of the decay curve of the polarization difference. These rates can be associated with the intra and intermolecular NH_3^+–CH_3 nearest proton–proton distances in crystalline alanine [46].

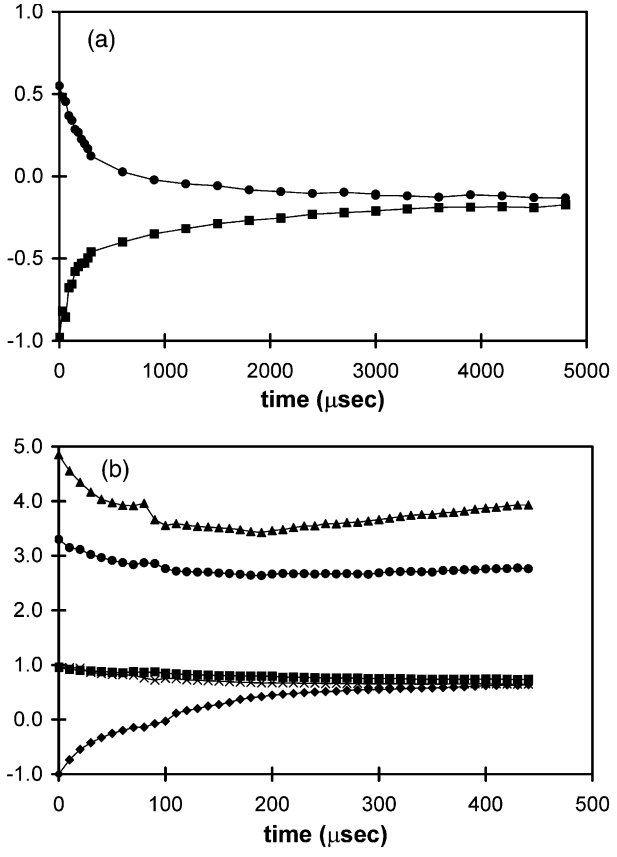

Fig. 5. Results of proton spin diffusion measurements on 2-[^{2}H]alanine and NA-histidine are depiced in (a) and (b), respectively. The pulse sequence in Fig. 1b with increasing spin diffusion time was used to collect the integrated intensities of the resolved proton bands in the two samples. In (a) the NH_3^+ protons were initially inverted. These intensities of the two lines in the proton spectrum were normalized to the initial intensity of the inverted line. In (b) the –NH(4) (diamonds) line of NA-histidine was inverted initially and the integrated intensities of the spectral bands corresponding to –NH(2) (squares), H_2O (X'es), {–CH(3), –CH(5), NH_3^+} (triangles) and {α-CH, β-CH_2} (circles) are plotted as a function of spin diffusion time. The H_2O and the {α-CH, β-CH_2} line intensities were obtained by a Gaussian line deconvolution.

A similar experiment was performed on a polycrystalline sample of natural abundant histidine, with an initial inversion of the –NH(4) ring proton. The results of the internal equilibration process are shown in Fig. 5b. In the natural abundant sample the proton–proton spin diffusion as well as the *w*PMLG proton spectra are not influenced by heteronuclear ^{13}C–^1H interactions. As a result the *w*PMLG spectrum exhibits ^{12}CH and $^{12}CH_2$ proton lines that are narrower than the same lines in the U-histidine spectrum. This effect is clearly observed on the 2 ppm line and the shoulders of the 8 ppm line as shown in Fig. 6.

The initial time dependence of the integrated proton line intensities presented in Fig. 5b demonstrates the initial equilibration process due to proton–proton spin diffusion. The signals are normalized by assigning a value of −1 to the inverted –NH(4) proton line intensity. The relative intensities at initial time and at final time are about equal to the number of protons in each band excluding the H_2O line. This line exhibits a lower intensity through the spin diffusion experiment that is similar to its value in the selective inversion experiment. Quantitative analysis of the rates of proton polarization redistribution in histidine require extensive calculations using multi-spin simulation program and is outside the scope of this publication.

In an additional set of experiments the protons were prepared in a selectively inverted state and locked along the LG off-resonance field in the tilted rotating frame. Their polarization was transferred to coupled carbon nuclei by means of a LGCP process. The pulse scheme of these experiments is given in Fig. 1c. Carbon spectra of U-histidine acquired after a selective DANTE-PMLG inversion and a LGCP period of 200.0 μs are shown in Fig. 7. The assignment of carbon lines is given in the top carbon spectrum in the figure [47]. The short LGCP contact time results in reduced intensity on the quar-

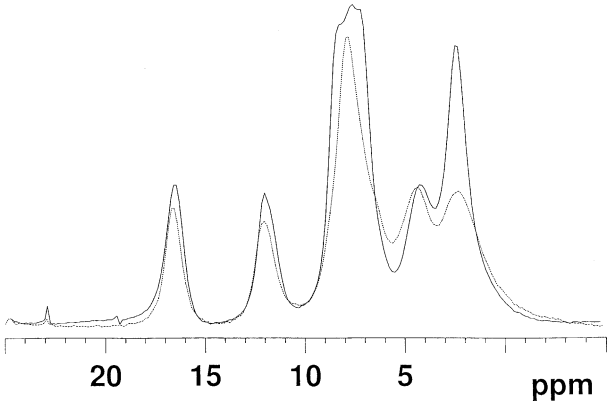

Fig. 6. A comparison between the *w*PMLG spectra of NA-histidine (solid line) and U-histidine (dotted line).

ternary ring and carboxyl carbon lines. For each DANTE-PMLG inversion experiment the proton carrier frequency during the LGCP interval was adjusted to a value that achieved maximal transfer of polarization from the inverted proton to the nearest carbon. In the insert at the top of the figure the positions of the carrier frequency during the DANTE-PMLG period are given by arrows pointing at the *w*PMLG proton spectrum. The 8 ppm line exhibits two hardly noticeable shoulders on both sides of the main intense NH_3^+ peak that are associated with the two CH ring protons. Experiments were performed at DANTE-PMLG carrier frequencies of 1000, 500, 0, −500, −1000 Hz relative to the frequency of the maximum of this line. The resultant ^{13}C spectra for these five experiments are plotted in Figs. 7a–e. The selectivity of the DANTE inversion is clearly demonstrated, in particular the correlation of the inversions at 500 and −500 Hz and the ring CH carbon lines at 136 and 118 ppm. The carbons with no directly bonded protons, i.e., the ring quarternary and the carboxyl carbon, are partially polarized by the inverted protons and their signals have reduced intensities. In Fig. 7f the C_α and C_β carbons, directly coupled to their inverted protons, appear with negative line intensities. Other lines are positive due to a predominant polarization by non-inverted protons. The total decrease in the proton intensities after the inversion process reflects itself in the reduced intensities of the carbon lines. Note that the spectroscopic selectivity of the inversion is improved when detected indirectly. It is possible to distingish between the ring carbons directly bound to protons with a chemical shift difference of less than 2 ppm. Thus it is possible to correlate protons with corresponding, directly bound, carbons in solids by means of this method. It is worthwhile to mention that the expected carbon polarizations after the LGCP period are also sensitive to the specific resonance offset of a polarizing proton, as was shown before [48]. Thus in quantitative analysis of the expected polarization state of the carbons in these experiments all parameters of the proton DANTE-PMLG preparation period should be taken into account. Yet, for spectral editing purposes, this approach provides an important tool to identify carbons and to correlate them with corresponding protons.

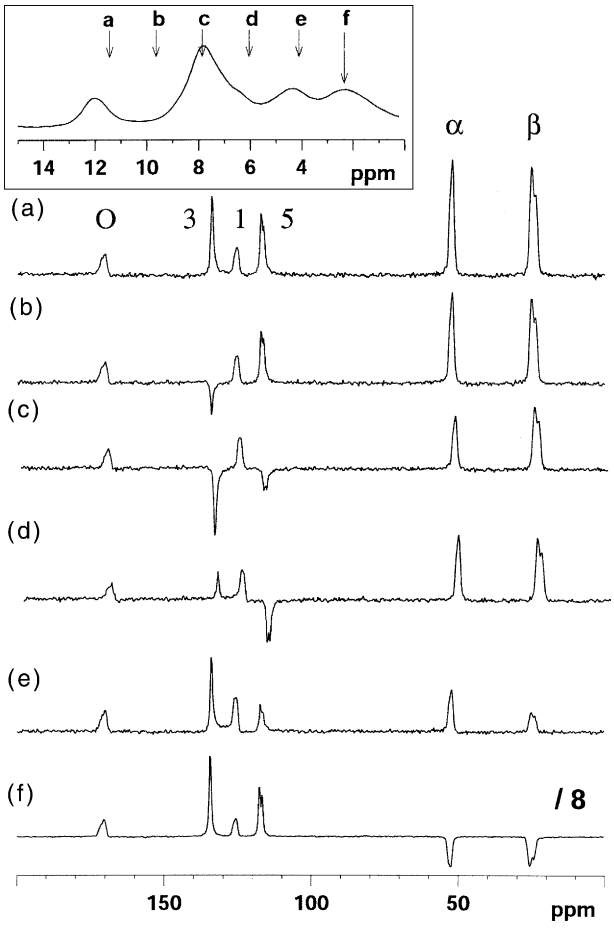

Fig. 7. U-histidine carbon spectra detected after selective proton line inversion using DANTE-PMLG at different carrier frequencies, followed by a proton–carbon Lee–Goldburg cross-polarization period of 200 μs as shown in Fig. 1c. Carbon lines of histidine are assigned as shown in (a). The values of the carrier frequency ν_H during the DANTE-PMLG inversion are indicated by arrows, pointing to specific positions in the *w*PMLG proton spectrum, inserted at the top of the figure. The (a–e) spectra were obtained for $\nu_H = -1000, -500, 0, 500$, and 1000 Hz, after 4 accumulations and (f) for $\nu_H = 1500$ Hz after 16 accumulations. These frequencies were measured with respect to the maximum in the proton spectrum at 8 ppm.

6. Conclusions

It has been shown that selective inversion of proton lines can be achieved by the DANTE-PMLG pulse sequence. The pulse scheme is robust, efficiently truncating the homogeneous broadening caused by dipolar interactions and enabling the inversion of individual lines in the proton spectra. Preparation of decoupled protons in a selectively inverted polarization state by using the DANTE-PMLG pulse scheme can be utilized to study different aspects of proton dynamics, e.g., heteronuclear CP spin exchange, chemical exchange, spin diffusion, and selective recoupling. Combining the DANTE-PMLG preparation with LGCP experiments can be used to obtain an accurate correlation of protons with their directly bonded low-abundant(X) spins, generating a spectral editing strategy. In many of these exepriments the *w*PMLG acquisition method is valuable for the design and optimization of complimentary pulse techniques and for the analysis of proton spectra and their dynamics in high resolution solid state proton NMR.

The DANTE-PMLG pulse sequence and a shape-file for the DRX/DSX Bruker spectrometers will be furnished upon request. They are available for download from our group website: http://www.weizmann.ac.il/chemphys/Vega_group/DANTE_PMLG.

Acknowledgments

The authors wish to thank US–Israel binational funding agency for its financial support.

References

[1] E.R. Andrew, A. Bradbury, R.G. Eades, Nature (London) 182 (1958) 1659.
[2] E.R. Andrew, A. Bradbury, R.G. Eades, Nature 183 (1959) 1802.
[3] I. Lowe, Phys. Rev. Lett. 2 (1959) 285.
[4] M.M. Maricq, J.S. Waugh, J. Chem. Phys. 70 (1979) 3300–3316.
[5] S. Hafner, H.W. Spiess, J. Magn. Reson. A 121 (1996) 160–166.
[6] A. Samoson, T. Tuherm, 1st Alpine Conference on Solid State NMR, Chamonix-Mont Blanc, France, 1999.
[7] M. Lee, W.I. Goldburg, Phys. Rev. A 140 (1965) 1261–1271.
[8] M. Mehring, J.S. Waugh, Phys. Rev. B 5 (1972) 3459.
[9] A. Bielecki, A.C. Kolbert, M.H. Levitt, Chem. Phys. Lett. 155 (1989) 341–346.
[10] A. Bielecki, A.C. Kolbert, H.J.M. de Groot, R.G. Griffin, M.H. Levitt, Adv. Magn. Reson. 14 (1990) 111.
[11] M.H. Levitt, A.C. Kolbert, A. Bielecki, D.J. Ruben, Solid State Nucl. Magn. Reson. 2 (1993) 151–163.
[12] E. Vinogradov, P.K. Madhu, S. Vega, Chem. Phys. Lett. 314 (1999) 443–450.
[13] E. Vinogradov, P.K. Madhu, S. Vega, J. Chem. Phys. 115 (2001) 8983–9000.
[14] J.S. Waugh, L.H. Huber, U. Haeberlen, Phys. Rev. Lett. 20 (1968) 180–182.
[15] P. Mansfield, J. Phys. C 4 (1971) 1444.
[16] W.K. Rhim, D.D. Elleman, R.W. Vaughan, J. Chem. Phys. 59 (1973) 3740.
[17] D.P. Burum, W.K. Rhim, J. Chem. Phys. 71 (1979) 944.
[18] J.T. Rasmussen, M. Howhy, H.J. Jakobsen, N.C. Nielsen, Chem. Phys. Lett. 314 (1999) 239.
[19] D. Sakellariou, A. Lesage, P. Hodgekinson, L. Emsley, Chem. Phys. Lett. 319 (2000) 253.
[20] D. Sakellariou, P. Hodgkinson, A. Lesage, L. Emsley, 30th Congress Ampere on Magnetic Resonance and Related Phenomena, Lisbon, 2000.
[21] R.E. Taylor, R.G. Pembleton, L.M. Ryan, B.C. Gerstein, J. Chem. Phys. 71 (1979) 4541.
[22] S.T. Dec, C.E. Bronnimann, R.A. Wind, G.E. Maciel, J. Magn. Reson. 82 (1989) 454.
[23] B.C. Gerstein, in: Encyclopaedia of NMR, Wiley, New York, 1996, p. 1501.
[24] L.M. Ryan, R.E. Taylor, A.J. Paff, B.C. Gerstein, J. Chem. Phys. 72 (1980) 508.
[25] S. Hafner, H.W. Spiess, Solid State Nucl. Magn. Reson. 8 (1997) 17–24.
[26] C. Filip, S. Hafner, J. Magn. Reson. 147 (2000) 250–260.
[27] E. Vinogradov, P.K. Madhu, S. Vega, Chem. Phys. Lett. 354 (3–4) (2002) 193–202.
[28] K. Yamauchi, S. Kuroki, I. Ando, J. Mol. Struct. 602–603 (2002) 9–16.
[29] G.A. Morris, R. Freeman, J. Magn. Reson. 29 (1978) 433–462.
[30] P. Caravatti, G. Bodenhausen, R.R. Ernst, J. Magn. Reson. 55 (1983) 88–103.
[31] C.A. Klug, W. Zhu, K. Tasaki, J. Schaefer, Macromolecules 30 (1997) 1734–1740.
[32] Y.K. Lee, N.D. Kurur, M. Helmle, O.G. Johannessen, N.C. Nielsen, M.H. Levitt, Chem. Phys. Lett. 242 (1995) 304–309.
[33] I. Schnell, A. Watts, Chem. Phys. Lett. 335 (2001) 111–122.
[34] D. Reichert, T. Mizuno, K. Takegoshi, T. Terao, J. Magn. Reson. 139 (1999) 308–313.
[35] A. Schmidt, S. Kababya, M. Appel, M. Botoshansky, S. Khatib, Y. Eichen, 41st Rocky Mountain Conference of Analytical Chemistry, Denver, Colorado, 1999.
[36] I.J. Lowe, R.F. Wysong, J. Magn. Reson. B 101 (1993) 106–109.
[37] D.P. Raleigh, M.H. Levitt, R.G. Griffin, Chem. Phys. Lett. 146 (1988) 71–76;
M.H. Levitt, D.P. Raleigh, F. Creuzet, R.G. Griffin, J. Chem. Phys. 92 (1990) 6347–6364.
[38] A.E. Bennett, J.H. Ok, R.G. Griffin, S. Vega, J. Chem. Phys. 96 (1992) 8624–8627.
[39] H.W. Spiess, Annu. Rev. Mater. Sci. 21 (1991) 131–158;
D.E. Demco, A. Johansson, J. Tegenfeldt, Solid State Nucl. Magn. Reson. 4 (1995) 13–38;
K. Schmidtrohr, ACS Symp. Ser. 598 (1995) 184–190.
[40] T. Fujiwara, A. Ramamoorthy, K. Nagayama, K. Hioka, T. Fujito, Chem. Phys. Lett. 212 (1993) 81–84;
M. Baldus, M. Tomaselli, B.H. Meier, R.R. Ernst, Chem. Phys. Lett. 230 (1994) 329–336;
T. Fujiwara, P. Khandelwal, H. Akutsu, J. Magn. Reson. 45 (2000) 73–83;
Y. Ishii, J. Chem. Phys. 114 (2001) 8473–8483.
[41] P. Caravatti, M.H. Levitt, R.R. Ernst, J. Magn. Reson. 68 (1986) 323–334.
[42] P. Caravatti, P. Neuenschwander, R.R. Ernst, Macromolecules 68 (1986) 323–334.
[43] J.D. Walls, M. Marjanska, D. Sakellariou, F. Castiglione, A. Pines, Chem. Phys. Lett. 357 (2002) 241–248.
[44] B.J. Van Rossum, C.P. de Groot, V. Ladizhansky, S. Vega, H.J.M. de Groot, J. Am. Chem. Soc. 122 (2000) 3465–3472.
[45] M. Bak, J.T. Rasmussen, N.C. Nielsen, J. Magn. Reson. 147 (2000) 296–330.
[46] D. Reichert, G. Hempel, R. Poupko, Z. Luz, Z. Olejniczak, P. Tekely, Solid State Nucl. Magn. Reson. 13 (1998) 137–148.
[47] B.Q. Sun, C.M. Rienstra, P.R. Costa, R. Willamson, R.G. Griffin, Am. Chem. Soc. 119 (1997) 8540–8546.
[48] V. Ladizhansky, E. Vinogradov, B.J. Van Rossum, H.J.M. de Groot, S. Vega, J. Chem. Phys., in press.